nature physics

LETTERS

https://doi.org/10.1038/s41567-018-0179-8

Pair-breaking quantum phase transition in superconducting nanowires

Hyunjeong Kim[1], Fédéric Gay[2], Adrian Del Maestro[3], Benjamin Sacépé[2] and Andrey Rogachev[1*]

Quantum phase transitions (QPT) between distinct ground states of matter are widespread phenomena[1–5], yet there are only a few experimentally accessible systems[6,7] where the microscopic mechanism of the transition can be tested and understood. These cases are unique and form the experimentally established foundation for our understanding of quantum critical phenomena. Here we report that a magnetic-field-driven QPT in superconducting nanowires—a prototypical one-dimensional system (d=1)—can be fully explained by the critical theory[8,9] of pair-breaking transitions characterized by a correlation length exponent $\nu \approx 1$ and dynamic critical exponent $z \approx 2$. We find that in the quantum critical regime, the electrical conductivity is in agreement with a theoretically predicted scaling function and, moreover, that the theory quantitatively describes the dependence of conductivity on the critical temperature, field magnitude and orientation, nanowire cross-sectional area, and microscopic parameters of the nanowire material. At the critical field, the conductivity follows a $T^{(d-2)/z}$ dependence predicted by phenomenological scaling theories[10,11] and more recently obtained within a holographic framework[12]. Our work uncovers the microscopic processes governing the transition: the pair-breaking effect of the magnetic field on interacting Cooper pairs overdamped by their coupling to electronic degrees of freedom. It also reveals the universal character of continuous quantum phase transitions.

Quantum phase transitions occur in many systems, including magnetic materials[1], superconductors[13–15], cold atomic gases[3] and also atomic nuclei[4] and stars[5]. Similar to the thermal fluctuations in classical temperature-driven phase transitions, strong quantum fluctuations near the critical point of a QPT lead to the emergence of universal long-range behaviour, which can be common in very diverse systems. However, for a complete description of a QPT one must also identify and quantitatively incorporate into a theory specific microscopic processes which drive a system across the critical point and induce the fluctuations. Examples where such complete theories can be experimentally tested are scarce and include the two-channel Kondo effect in quantum dots[7] and Luttinger liquid behaviour in materials composed of weakly coupled one-dimensional (1D) spin-chains[6].

Superconducting systems present special interest in the context of QPTs because the fluctuations near the critical point can lead to the formation of unconventional superconducting phases (most notably this is one of the scenarios for high-temperature superconductivity in the cuprates[16]). They also present a challenge—despite many years of efforts and overall success of phenomenological finite-size scaling analyses[2,13,14,17], the microscopic mechanism of QPTs in 2d superconductors is still debated. In contrast, the physics of a QPT becomes much more transparent in 1D superconductors. Here we show that essentially all long-range and microscopic characteristics of a QPT driven in superconducting nanowires by a magnetic field can be described by a pair-breaking critical theory.

A 1D superconductor can be defined as a wire with diameter smaller than $\pi 2^{1/2}\xi(0)$, where $\xi(0)$ is the zero-temperature Ginzburg–Landau coherence length[18]. This condition ensures that vortices do not form within the wire and that the superconducting order parameter is approximately constant at a given cross-section. 1D superconductors, as all 1D systems, are strongly affected by fluctuations, which can be both thermally activated or caused by quantum tunnelling[19–21]. The rate of fluctuations increases exponentially in thin wires.

Many experimental studies[22,23] have shown that reducing the nanowire diameter can drive a 1D superconductor into an insulating state. However, the microscopic mechanism of this process and the nature of the insulating phase (Bose insulator, Fermi insulator or some other state of matter) remains unclear. Better understood is the case when superconductivity is destroyed by a magnetic field[22,24]. Fig. 1 shows an expected phase diagram for this process.

The field acts on orbital and spin degrees of freedom of a Cooper pair as a pair breaker, cutting off the logarithmic divergence in the pairing susceptibility and setting a critical field B_c above which no bulk superconductivity is possible, even at $T=0$. At finite temperature, both the amplitude of the superconducting order parameter and the critical temperature are suppressed, as shown in the figure

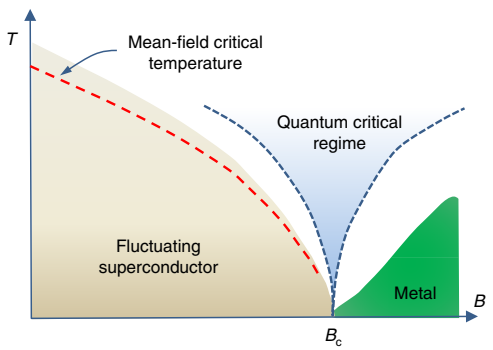

Fig. 1 | Schematic phase diagram for the pair-breaking superconductor to metal quantum phase transition in nanowires. The magnetic field dephases the effectively 1D Cooper pairs and suppresses the superconducting critical temperature to zero at a critical field B_c. In the quantum critical regime under consideration here, the existence of the quantum critical point results in large corrections to the nanowire conductivity due to superconducting fluctuations.

[1]Department of Physics and Astronomy, University of Utah, Salt Lake City, UT, USA. [2]Univ. Grenoble Alpes, CNRS, Grenoble INP, Institut Néel, Grenoble, France. [3]Department of Physics, University of Vermont, Burlington, VT, USA. *e-mail: rogachev@physics.utah.edu

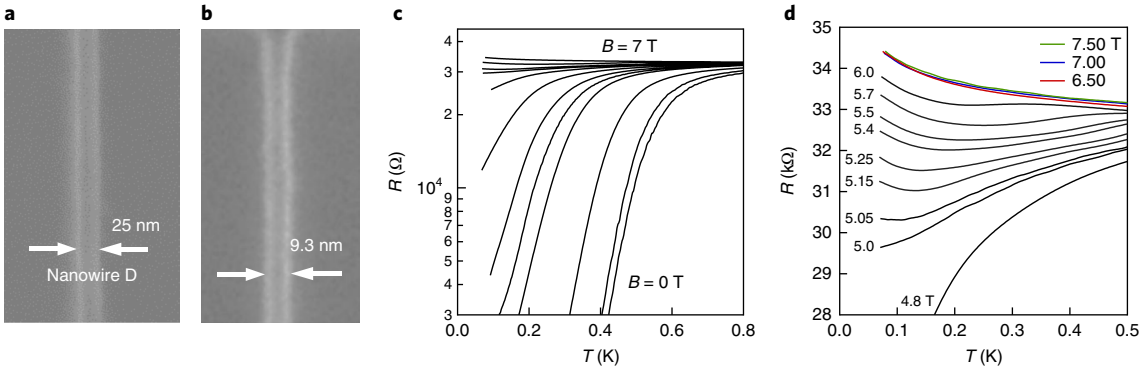

Fig. 2 | Superconductor–metal transition in nanowires. a, Scanning electron microscopy (SEM) image of nanowire D. **b**, SEM image of one of the thinnest fabricated nanowires (the wire was insulating in zero magnetic field and was not used in the present study), which demonstrates high uniformity of a nanowire's width achieved by the employed method. **c**, Resistance versus temperature for nanowire D in a parallel magnetic field in the range 0–7.50 T on a logarithmic scale. **d**, Same data on a linear scale near the critical field. Notice that the data at the fields 6.50, 7.00 and 7.50 T fall on top of each other, indicating complete suppression of superconducting fluctuations for these fields.

by the dashed line. Also, close to, but below B_c, the superconducting gap in nanowires shrinks to zero and the superconductivity becomes gapless; in this regime the superconducting condensate co-exists with normal quasiparticles. The state of the wire above B_c is, within the temperature range of our experiments, a normal disordered metal which experiences pairing fluctuations near the Fermi surface as a result of its proximity to the superconducting state. This can be pictured as a temporal conversion of a section of a wire into the superconducting state that leads to a measurable enhancement of the conductivity. Such corrections, due to both quantum and thermal fluctuations, were computed by Shah and Lopatin using a perturbative diagrammatic formalism[25]. The part of the phase diagram described by this theory is schematically shown in Fig. 1 in green.

In the simplest scenario, a quantum critical regime emerging between superconducting and metallic ground states should be controlled by microscopic processes present in the neighbouring phases. In this quantum regime, it was proposed that the behaviour of superconducting nanowires can be quantitatively described by a strongly coupled pair-breaking quantum field theory[8,9]. This theory captures the universal dynamics of strongly interacting fluctuating 1D Cooper pairs that are unable to form the condensate due to the existence of the magnetic field and that are overdamped (experience an effective frictional force) due to their interactions with a semi-infinite bath of uncondensed bulk electrons in the nanowire. Unlike theories that capture only phase fluctuations of the resulting superconducting order parameter, here amplitude fluctuations are also included in the dynamics. The resulting singular contribution to the conductivity due to superconducting fluctuations is predicted to take the scaling form

$$\sigma(T)=\frac{(e^*)^2}{\hbar}\left(\frac{\hbar D}{k_B T}\right)^{1/z}\Phi_\sigma\left(\frac{\hbar(\alpha-\alpha_c)^{\nu}}{k_B T^{1/z}}\right) \qquad (1)$$

where $e^*=2e$ is the charge of a Cooper pair, D is the diffusion coefficient, $\Phi_\sigma(x)$ is a dimensionless universal scaling function, α is the pair-breaking frequency and α_c its critical value, ν is the correlation length exponent and z is the dynamical exponent. The prefactor in equation (1) is a product of conductance, $(e^*)^2/\hbar$, and the thermal length, $L\sim T^{-1/z}$, the only available length scale of the problem which describes the size of a superconducting region of the nanowire. The prefactor represents the 1D case for the dependence $\sigma\sim T^{(d-2)/z}$ introduced from general considerations for the dynamic conductivity in the critical regime[10,11]. The same dependence is obtained from a class of holographic models using gauge–gravity duality[12]. The breakthrough aspect of the field theory that distinguishes it from earlier works on finite-size scaling analysis is that the entire function $\Phi_\sigma(x)$ is theoretically computed and therefore provides an unequivocal description of the critical regime of the QPT.

To verify the presence of the pair-breaking QPT in 1D superconductors we have studied a magnetic-field-driven transition in nanowires made of amorphous Mo–Ge alloys. Two studied nanowires, labeled E and D, had the same length, $L=3\,\mu$m, but different thickness, t, width, w, relative content of Mo and Ge, and as a result different T_c. (Nanowire E: $Mo_{78}Ge_{22}$, $t=6$ nm, $w=13$ nm, $T_c=1.5$ K; nanowire D: $Mo_{50}Ge_{50}$, $t=10$ nm, $w=25$ nm, $T_c=0.6$ K). Nanowires were fabricated using electron beam lithography with a negative resist; a scanning electron microscopy (SEM) image of nanowire D is shown in Fig. 2a. The method provided excellent uniformity of wires with very small variation of width, ±0.7 nm (Fig. 2b). Parameters of Mo–Ge alloys and nanowires are given in the Supplementary Information . For both nanowires, transport measurements were made in a parallel magnetic field and in a field transverse (perpendicular) to the long axis of the wire.

Figure 2c displays the temperature dependence of the resistance, $R(T)$, for nanowire D measured at low bias in a parallel magnetic field. At high fields (Fig. 2d) the $R(T)$ dependence first reveals a weak re-entrant behaviour and then, for $B\geq6.5$ T, becomes monotonic and field-independent. This behaviour indicates that fields above 6.50 T the superconducting fluctuations in the wire are completely suppressed. Qualitatively, the same variation was observed in a transverse magnetic field, and for nanowire E. In the high-field regime, the resistance follows the dependence expected for a normal 1D metal, $R_{HF}(T)=R_0+b/T^{\gamma}$, which contains the Drude and quantum correction terms. For nanowire E, $\gamma\approx0.5$, which corresponds to the correction caused by electron–electron interactions; for nanowire D a smaller value, $\gamma\approx0.27$, was found, probably because this wire is not strictly in the 1D regime for normal electrons ($w<L_T$). At high bias the wires display a positive zero-bias anomaly (not shown) due to electron heating [26].

The critical behaviour described by equation (1) is associated exclusively with superconducting fluctuations. However, the nanowire conductance also has a contribution from normal electrons, $G_N(T)$. As a first approximation, we assume that in the critical regime $G_N(T)$ does not change with the field and we take $G_N(T)=1/R_{HF}(T)$; the conductance of the superconducting channel is then determined as $G_S(T)=1/R(T,B)-G_N(T)$. Equation (1) indicates that $G_S(B)T^{1/z}$ versus B curves measured at different temperatures should cross at the critical field $B=B_c$. This crossing is indeed observed for nanowire D, as insets in Fig. 3a,b show, when we use the value $z\approx2$ predicted by the critical theory in the 'large-N' (N is

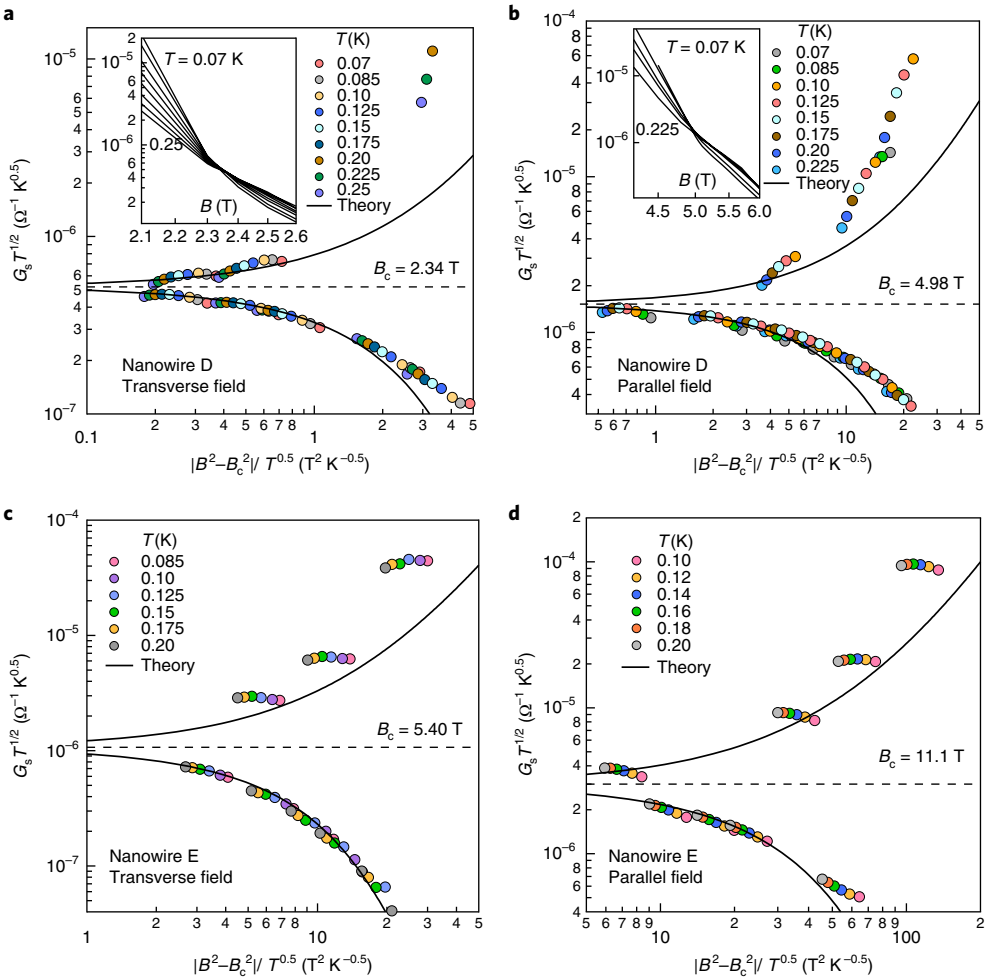

Fig. 3 | Finite-size scaling analysis. Conductance of the superconducting channel times $T^{1/2}$, $G_S T^{1/2}$, versus the scaling variable $|B^2-B_c^2|/T^{1/z\nu}$ (with the critical exponents product fixed to be $z\nu=2$) at different temperatures for nanowires E and D in parallel and transverse orientations of the magnetic field. The upper branch corresponds to the superconducting phase ($B < B_c$); the lower branch corresponds to the insulating phase ($B>B_c$). Each panel indicates the critical field, B_c. The solid lines indicate the prediction of the pair breaking critical theory. The inset to panel **a**,**b** shows $G_S T^{1/2}$ versus magnetic field.

number of components of the order parameter) limit[8,9]. Looking at Fig. 2d we notice that at the critical field, $B_c = 5.0$T, the resistance of the wire is 90% of its value in the normal state (at 7.5 T). This provides a posteriori justification of the approximation used to obtain $G_S(T,B)$. The value of the critical exponent $z\approx2$ predicted by the pair-breaking critical theory is distinct from the $z\approx1$ value typically associated with the Bose insulator state[2,10] that was observed experimentally in MoGe films[17] and 1D Josephson junction arrays[27].

The pair-breaking frequency α in 1D superconductors with strong spin–orbit scattering can be related to magnetic field as $\alpha=kB^2$, where the coefficient k contains both spin and orbital contributions and depends on the orientation of the field (see Supplementary Information for more details). We use this relation to verify the scaling behaviour predicted by equation (1) and plotted the quantity $G_S(B,T)T^{1/2}$ versus the scaling parameter $|B^2-B_c^2|/T^{1/z\nu}$. For both nanowires we obtained $G_S(B)$ from $R(T)$ curves measured at fixed fields. We found that for nanowire D, fixing the correlation length critical exponent to $\nu=1$ predicted by the pair-breaking theory[9] provides much better data collapse for both field orientations than the non-interacting value, $\nu=1/2$. Figure 3 displays the results. For nanowire E we did not detect a clear crossing in $G_S(B,T)T^{1/2}$ versus B curves. Nevertheless, we found that at certain value of B_c, a fairly good data collapse occurs on the insulating side of the transition (lower branch in Fig. 3). We give more comments on the quality of scaling below. The figure also indicates the critical fields for each data set; expectedly, B_c in the parallel orientation is substantially larger than in transverse one. For both nanowires the experimental values of B_c are quite close to their values estimated from mean field theory (see Supplementary Information for details); this indirectly supports our method of finding B_c for nanowire E.

The critical exponents are determined by the most general properties of a system, such as dimensionality and the symmetry of the order parameter. They can help to identify a universality class of a QPT, but by themselves do not provide much information about the microscopic physics of the transition. What markedly sets our work apart from the majority of studies of QPTs is the possibility to quantitatively compare experimental data with the critical theory, which predicts not only the exponents but also the scaling function itself, $\Phi_\sigma(x)$. The scaling function was computed numerically in ref. [9]. A brief summary of the theory is presented in the Methods section and the dependence of $\Phi_\sigma(x)$ on its argument in the Supplementary Information. First, the theory makes a universal prediction that, at the critical field, $\Phi_\sigma(x)\approx0.218$. Using experimental values of $G_S(B=B_c)T^{1/2}$ and estimated diffusion coefficients of $Mo_{78}Ge_{22}$ ($0.5\,cm^2\,s^{-1}$) and $Mo_{50}Ge_{50}$ ($0.45\,cm^2\,s^{-1}$) alloys (see Supplementary Information for details), we found that $\Phi_{\sigma\perp}(0)\approx0.16$ and $\Phi_{\sigma\parallel}(0)\approx0.46$ for nanowire E and $\Phi_{\sigma\perp}(0)\approx0.085$ and $\Phi_{\sigma\parallel}(0)\approx0.24$ for nanowire D, where the sub-index indicates the

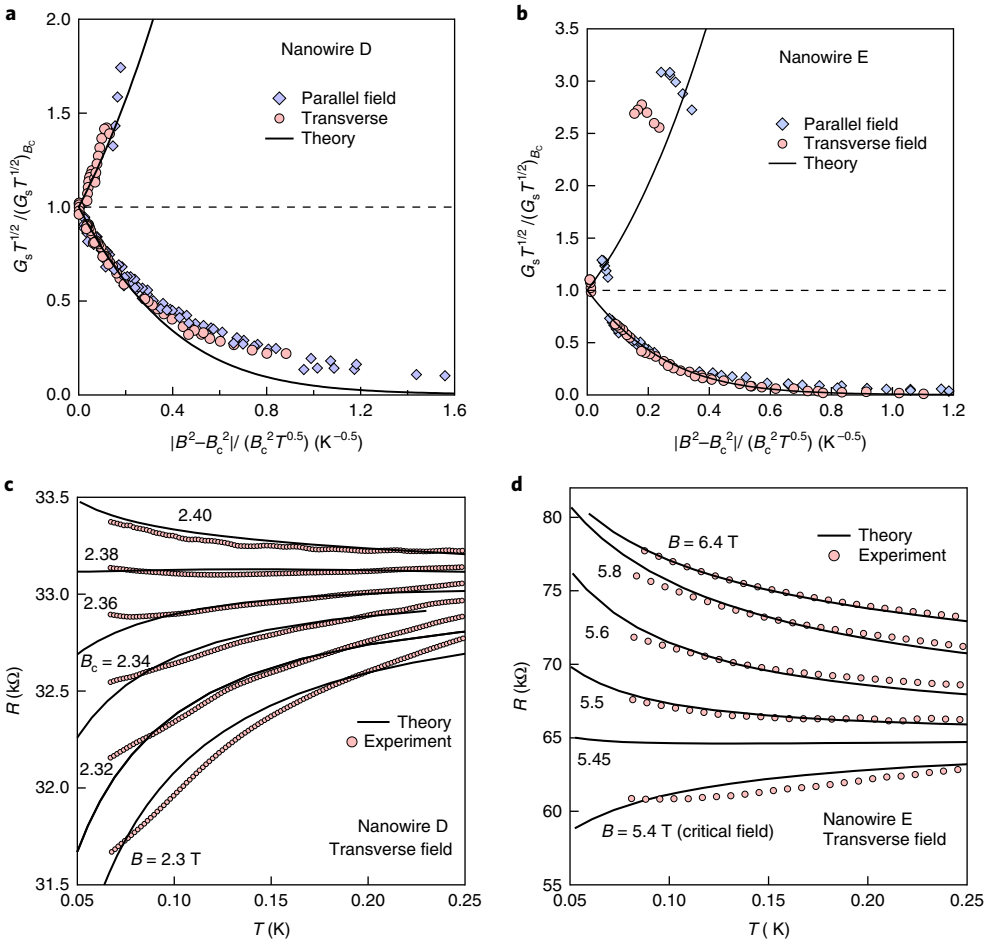

Fig. 4 | Quantitative test of the pair-breaking QPT theory. a,**b**, Conductance of superconducting channel times $T^{1/2}$, $G_S T^{1/2}$, normalized by its value at the critical field versus normalized scaling variable $|B^2-B_c^2|/T^{1/2}B_c^2$ for nanowires D (**a**) and E (**b**) in parallel and transverse field orientations. Black solid curves are predictions for the full scaling function in the quantum critical regime computed from the pair-breaking critical theory. **c**, Experimental $R(T)$ curves superimposed with $R(T)$ curves computed from the critical theory across the QPT for nanowire D in a transverse field. **d**, Same data for nanowire E in a transverse field in the insulating regime.

field orientation. The experiment reproduces the universal number within about a factor of two; this is remarkable given the simple approximation used for the extraction the conduction of the superconducting channel, uncertainty in the diffusion coefficient and the non-trivial prediction that at the critical field $\sigma \sim T^{(d-2)/z}$.

Another advantage of the pair-breaking QPT in 1D superconductors is that the phenomenological coupling parameters of the effective field theory can be connected to those of the microscopic Bardeen–Cooper–Schrieffer (BCS) theory. The details are given in the Methods; the final result is that the parameter of the scaling function can be written as

$$\Phi_\sigma(x) = \Phi_\sigma\left(C \times 0.54\left(\frac{\hbar k_B}{D}\right)^{1/2}(k_F\ell)^{1/2}\frac{A\sigma_{3d}T_c}{e^2}\frac{(B^2-B_c^2)}{B_c^2 T^{1/2}}\right) \qquad (2)$$

Here T_c, B_c, D, the cross section area A, and the bulk conductivity σ_{3d} are known nanowire parameters. The mean free path, ℓ, in amorphous Mo–Ge alloys is roughly equal to interatomic distance (0.3 nm); this assumption allows us to estimate the Fermi vector, k_F. The dimensionless constant C connects the bare and renormalized pair-breaking strengths and is the only adjustable parameter. Equation (2) allows us to test the analytical form of the scaling function and the relation of its argument to non-universal parameters characterizing a nanowire.

To make comparisons with the theory, in Fig. 4a,b we plot the quantity $G_S T^{1/2}$ normalized by its value at the critical field versus the normalized scaling variable $|B^2-B_c^2|/T^{1/2}B_c^2$. As predicted by equation (2) after normalization, the data for two field orientations coincide. The scaling function $\Phi_\sigma(x)$ is known from the theory in numerical form; we plotted it in the figure as $\Phi_\sigma(x)/\Phi_\sigma(0)$ and adjusted constant C to fit the data. Remarkably we found that for nanowire E, with $C \approx 0.05$ the theory matches the nonlinear variation of the data in the insulating regime (bottom branch in panel b). For nanowire D, the close value of the constant $C \approx 0.04$ also gives a good fit for both superconducting and insulating branches of the data, albeit in more narrow range of fields near B_c. The relatively small value of C could be indicative of possible deviations of the pair-breaking frequency from its mean-field value due to strong fluctuations near the QPT and also a multiplicative effect of small errors in microscopic parameters used in the scaling function argument. For completeness we plotted the theoretical predictions for the quantity $G_S T^{1/2}$ on top of each data set in Fig. 3.

With all parameters of the theory determined from the fit to the scaling function, we now reverse our analysis, and for each nanowire and field orientation use equations (1,2), and experimental conductance of the normal electrons, $G_N(T) = 1/R_{HF}(T)$, to compute theoretical $R_{th}(T)$ dependences corresponding to the series of the experimental $R(T)$ curves near the transition. The theoretical and experimental $R(T)$ dependences are shown in Fig. 4c,d.

We emphasize that all theory curves were generated with no additional adjustment; we used the values of C obtained from the scaling fit shown in Fig. 4a,b. So the overall agreement with the theory is remarkable. In Fig. 4d we added theoretical $R_{th}(T)$ for $B = 5.45$ T, which indicates that the weak reentrant behaviour, at least in principle, can be captured by the theory (more details are given in the Supplementary Information).

We further notice that the deviations from the theory for all data shown in Figs. 3 and 4 display a common trend. The agreement with the theory and the quality of the data scaling are the best in the insulating regime; however, they both become worse near the critical field and then even more so in the superconducting regime. The most likely reason is that with the evolution of a nanowire across B_c our approximation for the conduction of the normal channel, which is valid only in the perturbative limit, becomes progressively less accurate. Indeed, once superconducting fluctuations develop, the time-average density of normal electrons decreases. This should not only increase the temperature-independent Drude term in $R_N(T)$ but also alter its temperature dependence due to the modification of the quantum corrections. Apparently these effects are more significant in nanowire E, in which we did not observe the scaling of the conductance in the superconducting regime (Fig. 3c,d); only a general variation of $G_S T^{1/2}$ with the field follows the theory. This wire has roughly three times smaller cross-sectional area than nanowire D and a more pronounced $R_{HF}(T)$ dependence.

The agreement with the critical theory establishes that a quantum phase transition indeed takes place in 1D superconductors; this was not an obvious scenario to start with. Moreover, the fact that for both nanowires and field orientations the experiment reproduces the non-trivial dependence of the scaling function argument on several non-universal nanowire parameters, confirms that the theory accurately captures the microscopic physics at the transition. This allows us to draw several conclusions. The values of the exponents, ν and z, indicate strong interactions between superconducting fluctuations mediated by the normal electrons and validate the 'large-N' approximation used in the theory. This tells us that in the quantum critical regime the nanowire dynamically splits into semi-independent segments due to both phase and amplitude fluctuations that locally suppress the order parameter. The value of $z \approx 2$ and overall agreement with the pair-breaking critical theory allows us to rule out the unbinding of quantum phase-slip and anti-phase-slip pairs[19] as an alternative mechanism of the QPT. This later transition belongs to the 'phase-only' Berezinskii–Kosterlitz–Thouless (BKT) class and is claimed to occur in 1D Josephson-junction arrays[27]. A phase slip temporarily brings to a normal state a section of wire, which globally is in the superconducting state. In our case, in the quantum critical region shown in Fig. 1, both amplitude and phase fluctuations of the superconducting order parameters must be treated on equal footing due to the presence of the pair-breaking energy scale. The critical fluctuations responsible for the magnetic-field-driven QPT in nanowires microscopically are not phase slips, but Aslamazov–Larkin (AL)-type fluctuations[8,9,25], which produce superconducting regions in a normal metal. However, the AL theory must be modified in $d = 1$ to take into account the interactions between Cooper pairs overdamped due to their coupling to the fermionic quasiparticles of the proximate superconductor.

The obtained value of the critical exponent, $\nu \approx 1$, is in violation of the so-called Harris criteria for a disordered system, $\nu \geq 2/d$; that is, the system is effectively in a clean limit for the temperature range we consider where disorder acts on scales smaller than the thermal length (see Methods for more details).

Our findings are in accord with an earlier conjecture about the presence of dissipative effects in disordered superconducting films near the critical point[28]. A similarity between wires and films is expected since within perturbation theory[25] the microscopic effect of a magnetic field on both systems is the same. This suggests that a critical pair-breaking theory incorporating physical processes found to be relevant for nanowires may provide a not-yet-known microscopic description of QPTs in 2d disordered films of conventional superconductors. This approach can also be extended to describe a disorder-driven QPT in anisotropic gap superconductors where non-magnetic disorder acts as a pair-breaker. In fact, a theory[29] describing the behaviour of the magnetic susceptibility near a pair-breaking QPT in 2d films has been developed recently; a computation of conductivity within this theory is highly desirable for comparison with experiments. Future work can also explore a predicted correspondence between QPTs in superconducting nanowires and films and magnetic systems[30].

In summary, the excellent agreement with the quantum critical theory observed across the superconductor–metal transition in MoGe nanowires supports its microscopic underpinnings and represents an important benchmark in the confirmation of universality at quantum phase transitions.

Methods

Methods, including statements of data availability and any associated accession codes and references, are available at https://doi.org/10.1038/s41567-018-0179-8.

Received: 16 August 2017; Accepted: 17 May 2018;
Published online: 09 July 2018

References

1. Steppke, A. et al. Ferromagnetic quantum critical point in the heavy-fermion metal $YbNi_4(P_{1-x}As_x)_2$. *Science* **339**, 933–936 (2013).
2. Marković, N., Christiansen, C. & Goldman, A. M. Thickness–magnetic field phase diagram at the superconductor–insulator transition in 2d. *Phys. Rev. Lett.* **81**, 5217–5220 (1998).
3. Zhang, X., Hung, C.-L., Tung, S.-K. & Chin, C. Observation of quantum criticality with ultracold atoms in optical lattices. *Science* **335**, 1070–1072 (2012).
4. Cejnar, P., Jolie, J. & Casten, R. F. Quantum phase transitions in the shape of atomic nuclei. *Rev. Mod. Phys.* **82**, 2155–2212 (2010).
5. Alford, M. G., Schmitt, A., Rajagopal, K. & Schäfer, T. Color superconductivity in dense quark matter. *Rev. Mod. Phys.* **80**, 1455–1516 (2008).
6. Lake, B., Tennant, D. A., Frost, C. D. & Nagler, S. E. Quantum criticality and universality scaling of a quantum ferromagnet. *Nat. Mater.* **4**, 329–334 (2005).
7. Potok, R. M., Rau, I. G., Shtrikman, H., Oreg, Y. & Goldhaber-Gordon, D. Observation of the two-channel Kondo effect. *Nature* **446**, 167–171 (2007).
8. Del Maestro, A., Rosenow, B., Shah, N., & Sachdev, S. Universal thermal and electrical transport near the superconductor–metal quantum phase transition in nanowires. *Phys. Rev. B* **77**, 180501 (R) (2008).
9. Del Maestro, A., Rosenow, B. & Sachdev, S. Theory of the pairbreaking superconductor–metal transition in nanowires. *Ann. Phys.* **324**, 523–583 (2009).
10. Fisher, M. P. A., Weichmann, P. B., Grinstein, G. & Fisher, D. C. Boson localization and the superfluid–insulator transition. *Phys. Rev. B* **40**, 546–570 (1989).
11. Damle, K. & Sachdev, S. Nonzero-temperature transport near quantum critical points. *Phys. Rev. B* **56**, 8714–8733 (1997).
12. Hartnoll, S.A., Lucas, A. & Sachdev, S. *Holographic Quantum Matter* (MIT Press, Cambridge, MA, 2018).
13. Bollinger, A. T. et al. Superconductor–insulator transition in $La_{2-x}Sr_xCuO_4$ at the pair quantum resistance. *Nature* **472**, 458–460 (2011).
14. Ovadia, M., Kalok, D., Sacépé, B. & Shahar, D. Duality symmetry and its breakdown in the vicinity of the superconductor–insulator transition. *Nat. Phys.* **9**, 415–418 (2013).
15. Stewart, M. D., Yin, A., Xu, J. M., & Valles, J. M. Superconducting pair correlations in an amorphous insulating nanohoneycomb film. *Science* **318**, 1273–1275 (2007).
16. Jin, K., Butch, N. P., Kirshenbaum, K., Paglione, J. & Greene, R. L. Link between spin fluctuations and electron pairing in copper oxide superconductors. *Nature* **476**, 73–75 (2011).
17. Yazdani, A. & Kapitulnik, A. Superconductor–insulating transition in two-dimensional a-MoGe thin films. *Phys. Rev. Lett.* **74**, 3037–3040 (1995).
18. Bezryadin, A. *Superconductivity in Nanowires* (Wiley, Weinheim, 2013).
19. Arutyunov, K. Yu, Golubev, D. S. & Zaikin, A. D. Superconductivity in one dimension. *Phys. Rep.* **464**, 1–70 (2008).
20. Sahu, M. et al. Individual topological tunnelling events of a quantum field probed through their macroscopic consequences. *Nat. Phys.* **5**, 503–508 (2009).

21. Li, P. et al. Switching currents limited by single phase slips in one-dimensional superconducting Al nanowires. *Phys. Rev. Lett.* **107**, 137044 (2011).
22. Kim, H., Jamali, S. & Rogachev, A. Superconductor–insulator transition in long MoGe nanowires. *Phys. Rev. Lett.* **109**, 027002 (2012).
23. Makise, K., Terai, H., Tominari, Y., Tanaka, S. & Shinozaki, B. Duality picture of superconductor–insulator transition on superconducting nanowire. *Sci. Rep.* **6**, 27001 (2016).
24. Ning, W. et al. Superconductor–insulator transition in quasi-one-dimensional single-crystal Nb_2PdS_4 nanowires. *Nano Lett.* **15**, 869–875 (2015).
25. Shah, N. & Lopatin, A. Microscopic analysis of the superconducting quantum critical point: Finite-temperature crossovers in transport near a pair-breaking quantum phase transition. *Phys. Rev. B* **76**, 094511 (2007).
26. Kim, H. & Rogachev, A. Zero-bias anomaly in homogeneously disordered MoGe nanowires undergoing superconductor–insulator transition. *Phys. Rev. B* **94**, 254436 (2016).
27. Kuo, W. & Chen, C. H. Scaling analysis of magnetic-field-tuned phase transition in one-dimensional Josephson junction array. *Phys. Rev. Lett.* **87**, 186804 (2001).
28. Mason, N. & Kapitulnik, A. Dissipation effect on the superconductor–insulator transition in 2d superconductors. *Phys. Rev. Lett.* **82**, 5341–5344 (1999).
29. Galitski, V. Nonperturbative microscopic theory of superconducting fluctuations near a quantum critical point. *Phys. Rev. Lett.* **100**, 127001 (2008).
30. Hoyos, J. A., Kotabage, C. & Voita, T. Effect of dissipation on a quantum critical point with disorder. *Phys. Rev. Lett.* **99**, 230601 (2007).

Acknowledgements

The authors thank N. Shah, B. Rosenow, S. Sachdev and O. Starykh for valuable comments. Nanowire fabrication was carried out at the University of Utah Microfab and USTAR facilities. A.R. acknowledges Université Grenoble Alpes and Institute Néel, where measurements were performed, for hospitality. This research was supported in part by the National Science Foundation under award numbers DMR-1611421 (A.R.) and DMR-1553991 (A.D.) and by the ERC Grant QUEST number 637815 (B.S.). A.D. performed a portion of this work at the Aspen Center for Physics, which is supported by NSF grant PHY-1607611.

Author Contributions

H.K. fabricated nanowires, A.R., B.S. and F.G. carried out measurements, A.R., B.S. and A.D. carried out data analysis and wrote the manuscript, A.R. conceived and coordinated the project.

Additional information

Supplementary information is available for this paper at https://doi.org/10.1038/s41567-018-0179-8.

Reprints and permissions information is available at www.nature.com/reprints.

Correspondence and requests for materials should be addressed to A.R.

Publisher's note: Springer Nature remains neutral with regard to jurisdictional claims in published maps and institutional affiliations.

Methods

Nanowire fabrication. The nanowires were fabricated using Si wafers covered with a 100 nm layer of SiN and cut in individual samples with size 6×9 mm^2. First, using optical photolithography, consequential deposition of Ti (20 nm) and Au (40 nm) films, and liftoff procedure we fabricated a pattern consisting of 12 electrodes and several markers. Next, we sputter deposited a layer of amorphous Ge (thickness 3 nm) followed (without breaking vacuum) by the sputter deposition of MoGe alloy. To make good electrical connection between pre-patterned Ti/Au electrodes and thin MoGe films, square pads (5×5 μm, thickness 30 nm) were placed in each contact area by positive electron beam lithography with PMAA resist and liftoff. After patterning contact pads, the sample was immersed in the 2.5 % water solution of TMAH (the developer for negative electron beam lithography) for clearing. In the next step the whole sample was spin coated with 35-nm-thick HSQ (hydrogen silsequioxane) layer. The specification of the solution is XR-1541 2 %; it was purchased from Dow Corning. The nanowire and film electrodes were patterned by electron-beam lithography in a Nova Nano 630 Scanning Electron Microscope. The accelerating voltage was 30 keV; the dosage was 400-600 μC cm^{-2} for electrode areas and 3-8 nC cm^{-1} for nanowire lines. The exposed pattern was developed in 2.5 % water solution of TMAH for 2 min to remove HSQ. The pattern was etched with reactive ion etching using SF_6 gas.

Transport measurements. Measurements were carried out in a dilution refrigerator equipped with a superconducting solenoid. The use of lossy miniature stainless steel coaxial cables, room-temperature feedthrough filters, and capacitance to ground mounted directly on the sample holder at low temperature enable one to preclude spurious saturation of low resistive states at the lowest temperature. All measurements were performed with lock-in amplifier techniques and high-input-impedance voltage amplifiers in the current-bias configuration (~0.1–0.5 nA).

Data analysis. The microscopic parameters of Mo–Ge alloys (density of states, carrier density, diffusion coefficient, elastic scattering time, spin–orbit scattering time, Fermi velocity, effective mass) were computed from the known (or approximated) conductivity, specific heat and mass density data. The details are given in the Supplementary Information. Some of the extracted parameters have previously been used to explain several phenomena in Mo–Ge nanowires[26,31] and films [32].

The analysis employed the scaling function computed in the theory[9] in a numerical form. In this section, we reproduce some of the relevant details from refs [8,9]. which allow us to connect the dimensionless argument of the scaling function in equation (1) with the microscopic parameters of the experiment as reflected in equation (2).

Pair-breaking theory. The starting point is an effective theory of repulsive Cooper pairs in one spatial dimension without charge conservation in the condensate due to the existence of a large bath of unpaired fermions. This picture is appropriate due to the large number of transverse conduction channels in the metallic nanowires, but may also generically apply to other systems with pair-breaking, such as anisotropic d-wave superconductors with nonmagnetic impurities[33]. The resulting quantum critical action for the ohmically damped complex Cooper pair order parameter $\Psi(z,\tau)$ is:

$$S=\int_0^L dz\int_0^{\hbar\beta} d\tau\left[D\,|\partial_z\Psi(z,\tau)|^2+\alpha\,|\Psi(z,\tau)|^2+\frac{u}{2}\,|\Psi(z,\tau)|^4\right]+\frac{\eta}{\hbar\beta}\sum_{\omega_n}\int_0^L dz\;|\omega_n|\,|\Psi(z,\omega_n)|^2 \tag{3}$$

where z is a coordinate along the wire, $\beta=1/k_BT$, ω_n a bosonic Matsubara frequency, $D=v_F\ell/3$ is the diffusion constant with v_F the Fermi velocity and ℓ is the mean free path. Interactions are parametrized by $u>0$, which is relevant in $d=1$ and a quantum phase transition at α_c can be tuned by altering the strength of the pair-breaking frequency α which can be connected to the physical magnetic field (see below). The dynamics of the Cooper pairs are subject to damping due to their decay into the metallic bath characterized by the parameter η and we have defined the Fourier transform in imaginary time as:

$$\Psi(z,\omega_n)=\int_0^{\hbar\beta} d\tau\;\Psi(z,\tau)e^{i\omega_n\tau} \tag{4}$$

Simple power counting at tree level gives the bare value of the dynamical critical exponent to be $z=2$.

Effects of disorder. In principle, both the diffusion constant and pair breaking in equation (1) can be random functions of position x along the wire. Disorder in α is related to fluctuations in the local density of states and is expected to be relevant at $T=0$ at the quantum-critical point as defined by the Harris criterion since $1\approx d\nu<2$. A systematic study of the strongly disordered theory is presented in ref. [34], but here we neglect this randomness, and are thus restricted to the quantum critical regime at temperatures above T_{dis} determined by equating the thermal length $L_T=\sqrt{\hbar D/(k_BT_{dis})}$ to a zero-magnetic field disorder length scale $\ell_{dis}\equiv\ell N_\perp$, where $N_\perp=2nA/k_F$ is the number of transverse metallic conduction channels and $A=tw$ is the cross-sectional area of the nanowire[35]. This sets:

$$T_{dis}=\frac{\hbar}{3\,k_BN_\perp^2\tau} \tag{5}$$

where $\tau=\ell/v_F$ is the elastic scattering time given in the Supplementary Information. Using estimates for non-interacting electrons we find $T_{dis}\approx 0.5$–2.5 mK, which is far below the base temperature of our experiment, confirming the irrelevance of disorder in our results.

Connection with microscopic parameters. As described in the main text, the nanowires have a background metallic conduction for $\alpha>\alpha_c$ due to $N_\perp$ channels which can be identified from the large field regime due to the complete suppression of superconducting fluctuations. An analysis of equation (3) predicts that all important couplings between bosons and fermions scale to universal values and the singular contribution to the conductance obeys the scaling form given in equation (1) (see refs [8,9] for details). The interactions between Cooper pairs in the field theory described by equation (3) can be handled in the limit where the number of components N of the complex order parameter Ψ is assumed to be large ($N=1$ in the physical case). This 'large-N' approach is analogous to a self-consistent mean field theory and becomes exact when $N\to\infty$. In this limit, interactions lead to a renormalization of an effective Gaussian theory where $z=2$ and $\nu=1$ take their bare values. The contributions of superconducting fluctuations to electrical transport can then be analysed via the quantum Kubo formalism and $\Phi_\sigma(x)$ can be evaluated numerically, where x is a dimensionless scaling variable:

$$x=C\left(\frac{\hbar D}{k_BT\eta}\right)^{1/2}\frac{\alpha-\alpha_c}{\hbar u} \tag{6}$$

and C is a non-universal constant related to a renormalization due to the interactions between Cooper pairs (see ref. [9] for details of the calculation and rescaling).

The critical pair-breaking frequency is related to the critical temperature and critical parallel and transverse magnetic fields for a particular wire as $\alpha_c=0.88kT_c/\hbar=\gamma_\parallel B_{c\parallel}^2=\gamma_\perp B_{c\perp}^2$, where γ depends on orientation[36] and also takes care of the spin pair-breaking[36]. (See Supplementary Information for more details). Using this we can re-write

$$\hbar(\alpha-\alpha_c)=\hbar\alpha_c\frac{\alpha-\alpha_c}{\alpha_c}\simeq 0.88\;k_BT_c\frac{(B^2-B_c^2)}{B_c^2} \tag{7}$$

The remaining microscopic parameters u and η can be found from the following relations of BCS and time-dependent Ginzburg–Landau theory[37,38]:

$$\eta=\frac{\pi^2\hbar^2}{2\,m\,\xi^2(0)}\frac{1}{8k_BT_c}\simeq\frac{1.5}{k_F\ell} \tag{8a}$$

$$b=\frac{\hbar^2}{m\,\xi^2(0)n}\frac{1}{\chi(0.882\xi_0/\ell)} \tag{8b}$$

$$u=\frac{b}{A\hbar^2\eta^2}\simeq 1.33\frac{e^2D}{\sigma_{3d}A\hbar^2} \tag{8c}$$

where $\xi(0)=0.85\sqrt{\xi_0\ell}$ is the zero-temperature Ginzburg–Landau coherence length, $\xi_0=0.18\hbar v_F/k_BT_c$ is the Pippard coherence length and $\chi(0.882\xi_0/\ell)=1.33\,\ell/\xi_0$ is the Gor'kov function. Using the standard equations for the Drude conductivity and combining all terms we find

$$\Phi_\sigma(x)=\Phi_\sigma\left(C\times 0.54\left(\frac{\hbar k_B}{D}\right)^{1/2}(k_F\ell)^{1/2}\frac{A\sigma_{3d}T_c}{e^2}\frac{(B^2-B_c^2)}{B_c^2T^{1/2}}\right) \tag{9}$$

which appears in equation (2). The non-universal microscopic constant C is the only adjustable parameter in the theory and it can be extracted by fitting the scaling function to experimental data in the quantum critical regime. This parameter reflects not only the renormalization in the critical pair breaking frequency α_c due to interactions between Cooper pairs, but also the approximations used when matching the coupling constants in the effective field theory to microscopic values via the time-dependent Ginzburg–Landau theory. Perhaps a better quantitative

agreement with the theory can be reached if mesoscopic fluctuations of parameters are incorporated into Ginzburg–Landau functional[39].

Data Availability Statement. The data that support the plots within this paper and other findings of this study are available from the corresponding author upon reasonable request.

References

31. Rogachev, A., Bollinger, A. T. & Bezryadin, A. Influence of high magnetic fields on the superconducting transition of one-dimensional Nb and MoGe nanowires. *Phys. Rev. Lett.* **94**, 017004 (2005).
32. Kim, H. et al. Effect of magnetic Gd impurities on the superconducting state of amorphous Mo-Ge thin films with different thickness and morphology. *Phys. Rev. B* **86**, 024518 (2012).
33. I. F. Herbut, I. F. Zero-temperature *d*-wave superconducting phase transition. *Phys. Rev. Lett.* **85**, 1532–1535 (2000).
34. Del Maestro, A., Rosenow, B., Müller, M. & Sachdev, S. Infinite randomness fixed point of the superconductor–metal quantum phase transition. *Phys. Rev. Lett.* **101**, 035701 (2008).
35. Thouless, D. J. Maximum metallic resistance in thin wires. *Phys. Rev. Lett.* **39**, 1167–1169 (1977).
36. Lopatin, A. V., Shah, N. & Vinokur, V. M. Fluctuation conductivity of thin films and nanowires near a parallel-field-tuned superconducting quantum phase transition. *Phys. Rev. Lett.* **94**, 037003 (2005).
37. Tinkham, M. *Introduction to superconductivity* 2nd edn (Dover, Mineola, 1996).
38. Tucker, J. R. & Halperin, B. I. Onset of superconductivity in one-dimensional systems. *Phys. Rev. B* **3**, 3768–3781 (1971).
39. Konig, E. J. et al. Berezinskii–Kosterlitz–Thouless transition in homogeneously disordered superconducting films. *Phys. Rev. B* **92**, 214503 (2015).